Int J Earth Sci (Geol Rundsch) (2016) 105:2273–2284
DOI 10.1007/s00531-015-1287-7

ORIGINAL PAPER

Tithonian age of dinosaur fossils in central Patagonian, Chile: U–Pb SHRIMP geochronology

Manuel Suárez[1] · Rita De La Cruz[2] · Mark Fanning[3] · Fernando Novas[4] · Leonardo Salgado[5]

Received: 30 August 2014 / Accepted: 7 December 2015 / Published online: 28 December 2015
© Springer-Verlag Berlin Heidelberg 2015

Abstract Three Tithonian concordant U–Pb SHRIMP zircon ages of 148.7 ± 1.4, 147.9 ± 1.5 and 147.0 ± 1.0 from tuffs intercalated in a clastic sedimentary succession with exceptional dinosaur bones including the new taxon *Chilesaurus diegosuarezi* gen. et sp. nov. exposed in central Chilean Patagonia (ca. 46°30′S) are reported herein. The fossiliferous beds accumulated in a synvolcanic fan delta reaching a shallow marine basin as indicated by glauconite present in some of the beds, and coeval with the beginning of the transgression of the Aysén Basin.

Keywords U–Pb · Tithonian · Dinosaurs · *Chilesaurus diegosuarezi* gen. et sp. nov. · Patagonia · Chile

Introduction

The contribution of this article is in giving the analytical data of a zircon U–Pb SHRIMP Tithonian age for the host rocks of exceptional dinosaur fossil bones found by the authors in Chilean Patagonia in 2004 and exposed approximately at 1400 masl in the mountains south of the village of Mallín Grande, south of Lago General Carrera (Fig. 1; ca. 46°30′S; De la Cruz and Suárez 2006; Salgado et al. 2008; Novas et al. 2014). Well-known dinosaur fossils from Patagonia have so far been mainly restricted to Argentina and to the Cretaceous, with the exception of those found in the Jurassic Cañadón Asfalto basin, in northern Patagonia.

The Aysén fossil assemblage reported in this article includes theropod dinosaurs (Salgado et al. 2008; Novas et al. 2014, 2015), remains of sauropod dinosaurs and crocodiles (Novas et al. 2014; Lio et al. 2011). Late Jurassic theropods are very scarce in the southern hemisphere, with only a few known from Africa, and this discovery represents one of the first finds of Late Jurassic tetanuran theropods from the southern hemisphere (Salgado et al. 2008). Also these fossils are the first important collection of dinosaurs from Chile, one of the few findings with clearly Late Jurassic dinosaur fossil bones in South America (see Salgado et al. 2008) and the first Jurassic dinosaurs from Chile (Casamiquela et al. 1969; Salinas et al. 1991; Iriarte et al. 1999; Rubilar 2003). However, its main importance is due to the identification of *Chilesaurus diegosuarezi* gen. et sp. nov., a new taxon of theropod, that does not correspond to any previously documented taxon from the Mesozoic units of Patagonia or from the rest of the world, which represents a new lineage of theropod dinosaurs (Novas et al. 2015). The paleontological results are published elsewhere (Novas et al. 2015). "The new dinosaur… possesses an ankle and foot resembling those of basal sauropodomorphs, a forelimb with basal tetanuran features, and a pelvis similar to ornithischians and derived theropods. This combination of features departs from those recognized in any major dinosaur clade and represents an extreme example of mosaic

✉ Manuel Suárez
suarezpatagonia@yahoo.com; manuel.suarez@unab.cl

1 Carrera Geología, Facultad Ingeniería, Universidad Andres Bello, Sazie, 2315 Santiago, Chile

2 Servicio Nacional de Geología y Minería, Avenida Santa María, 0104 Santiago, Chile

3 Research School of Earth Sciences, The Australian National University, Canberra, CT 0200, Australia

4 Museo Argentino de Ciencias Naturales, Buenos Aires, Argentina

5 Consejo Nacional de Investigaciones Científicas y Técnicas (Conicet), Instituto de Investigación en Paleobiología y Geología, Universidad Nacional de Río Negro, Av. Gral. J.A. Roca 1242, 8332 General Roca, Río Negro, Argentina

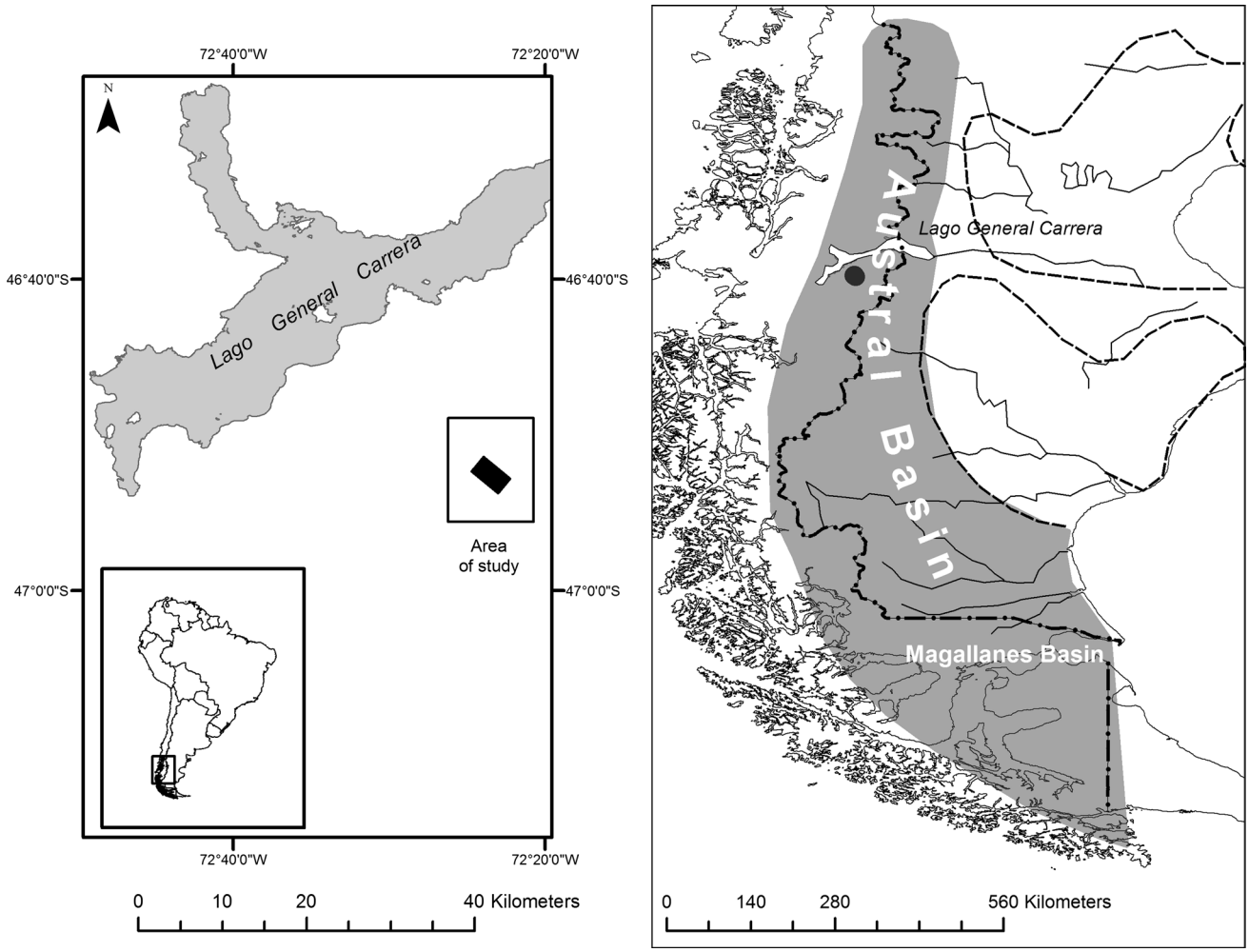

Fig. 1 Location map and geographic distribution of Austral Basin (from Bell and Suárez 1997)

convergent evolution. *Chilesaurus* is the most abundant reptile in the fossil assemblage in which it occurs, showing that this theropod was a main herbivorous consumer in this Late Jurassic southwestern Gondwanan tetrapod community" (Novas et al. 2015).

The fossil bones are incorporated in a succession of sandstones and conglomerates chronostratigraphically correlated with the Toqui Formation, which north of the study area represents the Tithonian–Berriasian diachronous transgression of the Aysén Basin or Río Mayo Embayment (Aguirre-Urreta and Ramos 1981; Bell and Suárez 1997) that forms the northern part of the Austral Basin, an oil-producing back-arc basin developed in southernmost South America (Fig. 1) in central western Patagonia (Suárez et al. 2009). The presence of tuffs interbedded in the clastic succession with dinosaur fossils gave an excellent and rare opportunity for zircon U–Pb dating of the beds containing these fossils. In this article we present U–Pb SHRIMP dates of three of the silicic tuffs interbedded with the dinosaur-bearing beds that give a Tithonian age. These dates were previously reported in a geological map of the area (De La Cruz and Suárez 2006), but the analytical data have not been published before. This work complements the paleontological studies that the authors have published elsewhere (Salgado et al. 2008; Novas et al. 2014, 2015).

The geological setting

The Mesozoic geological record of central Patagonian cordillera in the Aysén region of Chile (44–47°S) includes three main volcanic episodes starting in the Late Jurassic and the development of an intra- and back-arc marine basin during Tithonian to Aptian times known as Aysén basin (Figs. 1, 2, 3). The first volcanic episode is represented by the Ibáñez Formation, a mainly subaerial silicic volcanic unit of ?Oxfordian to Valanginian age (see Suárez et al. 2009), unconformably accumulated

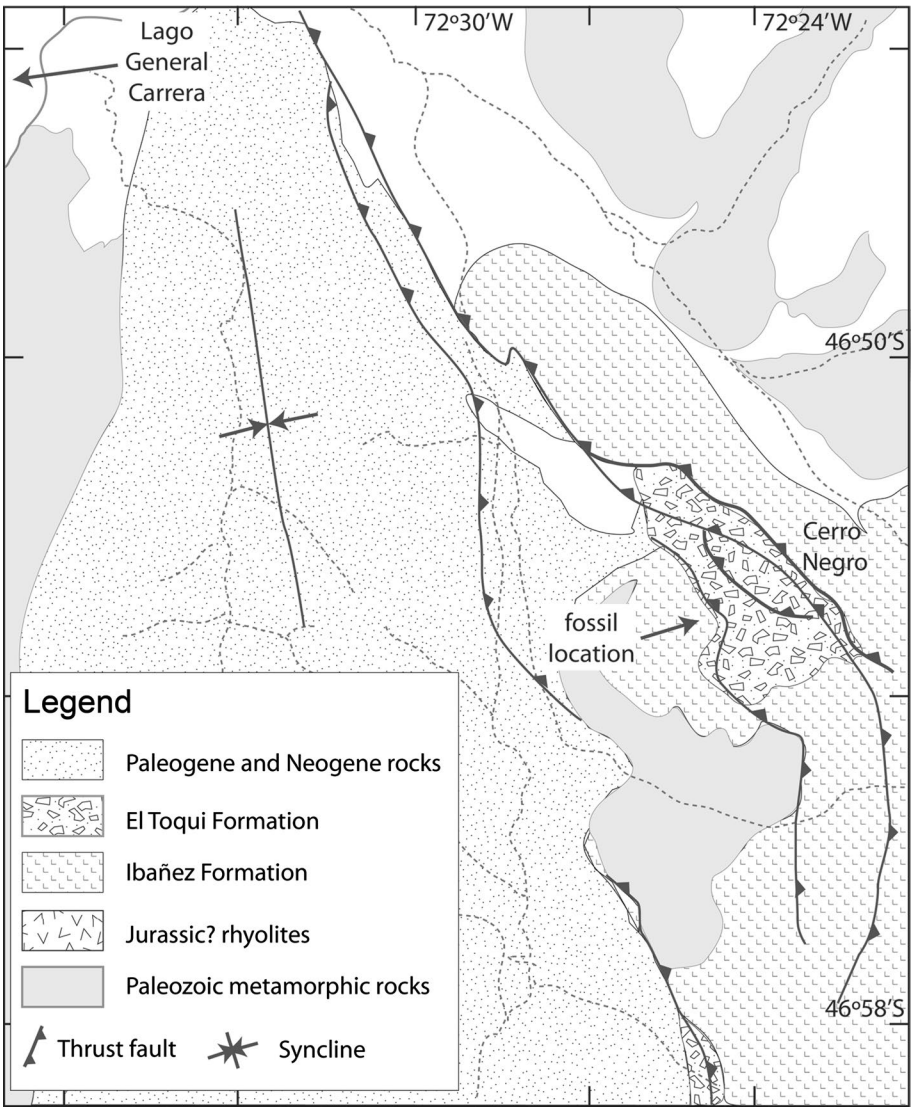

Fig. 2 Geologic scheme (modified from De La Cruz and Suárez 2006)

over Upper Paleozoic metamorphic rocks of the Eastern Andean Metamorphic Complex. The second volcanic episode is represented by the Aptian-early Cenomanian Divisadero Group, formed mainly by subaerial intermediate volcanic rocks (see De La Cruz et al. 2003; Suárez et al. 2014), and the third volcanic episode is represented by a Santonian–Danian group of volcanic rocks including andesites, rhyolitic domes and basalts (Casa de Piedra Volcanic Complex, El Toro Formation and Morro Negro Basalts); the andesitic and dacitic lava flows of the El Toro Formation unconformably overly ignimbrites of the Divisadero group (De La Cruz et al. 2003; Demant et al. 2007). The Aptian to Upper Cretaceous volcanic rocks are not represented in the area of this study, where tuffs conformably overlying the dinosaur-bearing succession are unconformably overlain by fluvial deposits of the Late Paleocene–Early Eocene Ligorio Márquez Formation (De La Cruz and Suárez 2006).

The Mesozoic marine sedimentary succession is represented by the Toqui, Katterfeld and Apeleg formations of the Coyhaique Group and deposited in the Aysén Basin. The Toqui Formation north of the studied area is composed of shallow marine sandstones, oyster beds and volcaniclastic rocks, and represents the Tithonian to early Hauterivian diachronous transgression of the basin. It overlies and interfingers with volcanic rocks of the Late Jurassic–Early Cretaceous Ibáñez Formation (De La Cruz et al. 2003; De La Cruz and Suárez 2006, 2008; Suárez et al. 2009). The Toqui Formation, north of lago General Carrera, is overlain by marine black shales of the Katterfeld Formation that underlie marine sandstones, mainly of tidal facies, of the Apeleg Formation (Bell and Suárez 1997). The latter underlies Aptian to Cenomanian subaerial volcanic rocks, mainly pyroclastic, of the Divisadero Group and locally Aptian surtseyan tuffs of the Baño Nuevo Volcanic Complex (Suárez et al. 2007, 2010; Demant et al. 2010).

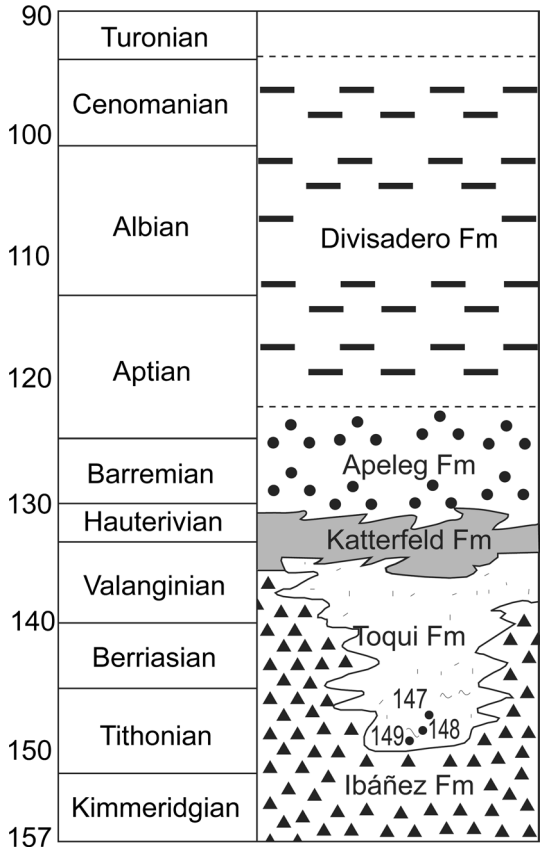

Fig. 3 Schematic Mesozoic stratigraphy

The dinosaur beds

The dinosaur beds crop out along the eastern side of a major NS Cenozoic syncline and are bounded to the east by west-vergent NNW thrusts (De la Cruz and Suárez 2006). To the west they form the hanging wall of a NS west-verging thrust over Upper Paleocene-Lower Eocene fluvial beds of the Ligorio Márquez Formation that in turn unconformably overlie the Ibáñez Formation (De La Cruz and Suárez 2006). Along a segment of one of the western thrusts, Upper Paleozoic rocks and Mesozoic rocks of the Ibáñez Formation are thrust over Miocene strata of the Santa Cruz Formation with a left-lateral strike-slip component (the Santa Elcira Thrust of De la Cruz and Suárez 2006), indicative of a post-16 Ma age for that particular fault. Farther to the east of the fossiliferous beds, west-vergent thrusts occur, where Upper Paleozoic metamorphic rocks are thrust over the Jurassic-Lower Cretaceous Ibáñez Formation uplifting the cordilleran segment to the east after or during the latest stages of deposition of the Santa Cruz Formation.

The dinosaur beds are weakly folded and faulted. Several faults putting in contact beds of the same facies association can be identified, mainly interpreted as thrusts based on few fault striae and the folding of the beds (see De La Cruz and Suárez 2006); however, normal faults have also been identified.

Lithology

The fossiliferous sedimentary unit is a sandstone, pebbly sandstone, conglomerate succession, with intercalated tuffs and tuffites composed of reworked pyroclastic debris, that can be divided into two main facies associations: (1) a lower facies association of gray beds directly overlying ignimbrites of the Ibáñez Formation, and (2) an upper facies association, of green color, with reddish tones, and with intercalated tuffs and tuffites (Figs. 4, 5), underlying a thick succession of red-colored ignimbrites of over 50 m thick. Most of the fossil collections and geological observations were made from parts of the upper green facies, although fossil bones were also observed at least in the uppermost beds of the lower facies association. Clasts are mainly volcanic, with metamorphic fragments more abundant in the lower facies. No plutonic fragments were identified.

The lower facies association, of approximately 60 m thick, includes matrix-supported conglomerates, interpreted as debris flow deposits, clast-supported fine-grained normally graded conglomerates, interpreted as deposits from a turbulent flow, tuffaceous sandstones, laminated fine and very fine-grained sandstones and siltstones interpreted as subaqueous, laminated and finely stratified beds with concentrations of pumices probably representing water-lain air-fall deposits. Soft sediment deformation occurs occasionally (flames and sandstone dikes), indicative of rapid accumulation of sediments. Some beds are mainly composed of rhyolite and metamorphic clasts, while in others the clasts are predominantly of schists and metamorphic quartz, with subordinate volcanic fragments. They are interpreted as alluvial fan and lacustrine facies. A zircon U–Pb SHRIMP date was obtained from a vitric tuff from the uppermost levels (sample CH-8199).

The upper facies association: of approximately 70 m thick of medium to thin bedded strata, was more thoroughly explored for fossils (Salgado et al. 2008; Novas et al. 2014, 2015). Two zircon U–Pb SHRIMP dates from intercalated tuffs were obtained from this association (samples CH-6281 and CH-8177). The upper green-reddish succession is formed of alternating green pebbly sandstones and sandy sedimentary conglomerates and breccias, with intercalated red or brown tuffs and tuffaceous rocks (Fig. 4). The contacts between beds are frequently erosional and paleochannels and cut and fill structures are common.

The intercalated tuffs include a distinctive red vitric tuff more than 15 m thick with *fiamme* up to 2 cm in length and interpreted as an ignimbrite (sample CH-6281 was taken from it), brown tuffs and tuffites, less than 2 m in thickness

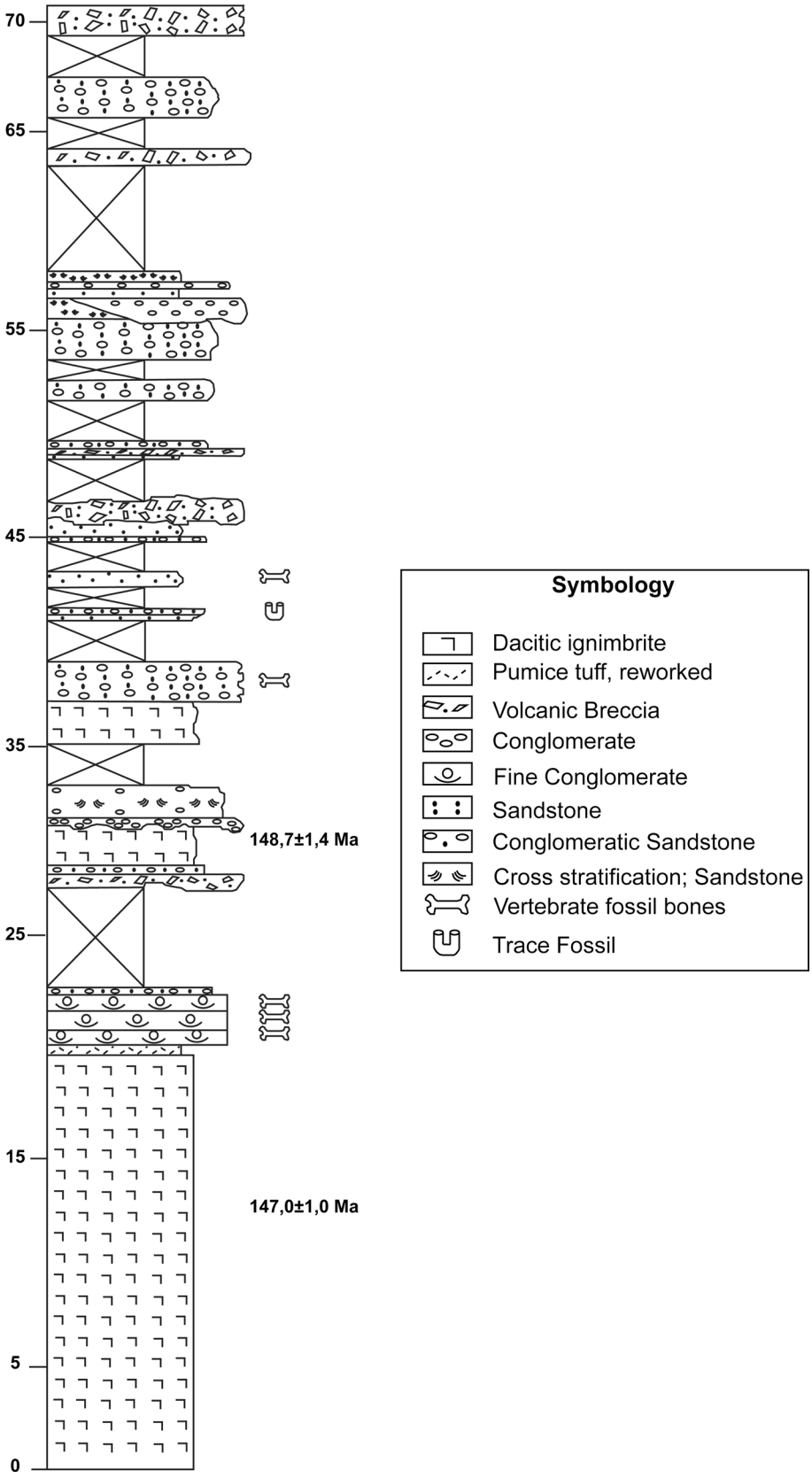

Fig. 4 Stratigraphic column of dinosaur-bearing beds, Toqui Formation

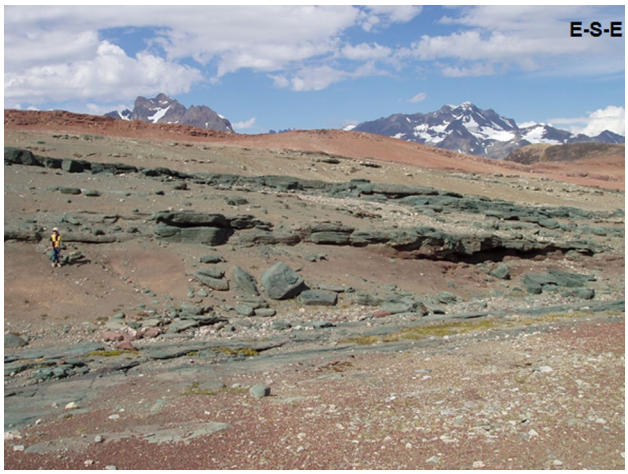

Fig. 5 Green sandstones and breccias with intercalated reddish tuffs

and usually with eroded tops. Laminated and finely stratified tuffs with green fragments of pumice less than 1 cm in diameter and with horizontal and vertical trace fossils are interpreted as water-lain air-fall tuffs.

The sandstones are coarse-grained and poorly sorted, frequently grading to pebbly sandstones and granule conglomerates. They are mainly formed by fragments of andesites, rhyolites, dacites, basalts, quartzites, micaceous schists, plagioclase and rare quartz. Green volcanic fragments give the color to the sandstones and conglomerates.

The conglomerates and breccias, both matrix and clast supported, are very poorly sorted with clasts from millimeters to over 60 cm in diameter and exhibit crude clast subparallel alignment. Most clasts are volcanic in origin, including tuffs, volcanic breccias, dacites and andesites, and occasional metamorphic quartz.

The sedimentary structures observed in the sandstones include upper flat beds, locally with current lineation, planar and trough cross bedding and in the conglomerates rare localized imbrication of clasts. Some granule conglomerates and pebbly sandstones, 10–20 cm in thickness, are massive, structureless or with normal grading; usually they include outsize clasts of up to 60 cm in diameter. The breccias and conglomerates represent debris flow and stream flow deposits. The matrix-supported conglomerates may represent reworking of previously rounded fragments by fluvial processes. Monomictic debrites with rounded rhyolite clasts up to 15 cm in diameter can be interpreted as the product of the reworking of block and ash deposits by debris flows.

A distinctive facies within this association is that of four-meter-thick laminated fine-grained quartz-feldspar sandstones, of gray color, capped by a millimeter thick claystone laminae, and with *Paleophycus* or *Planolites* trace fossils (Eduardo Bellosi, photographic identification, written comm. 2014) and abundant detrital biotite and scarce fossil bones.

Some of the green sedimentary beds are interpreted as marine due to the presence of glauconite (Poldie Oyarzún, Universidad Andres Bello X Ray Diffractometry Laboratory, written communication, 2014). Glauconite was previously reported from samples from other beds of the green upper facies association (Sernageomin X Ray Diffractometry Laboratory, 2006, written communication in De La Cruz and Suárez 2006). However, analyses carried out in other green color sandstones do not show glauconite but chamosite and celadonite. The cement is calcite and locally chlorite and hematite/limonite.

The presence of tractive structures, debrites and water-lain fall tuffs, probably shallow marine based on the presence of glauconite in some beds, suggests fan delta deposits in an active volcanic arc setting, reaching a shallow marine environment.

The fossils

The fossils discovered in the exposures assigned to the Toqui Formation south of Lago General Carrera in the Aysén Region of Chilean Patagonia include dinosaurs (Salgado et al. 2008; Novas et al. 2014), a new taxon named *C. diegosuarezi* (Novas et al. 2015) and crocodiles (Lio et al. 2011), locally fossil tree trunks of *Podocarpoxylon* and trilete spores (fern) that indicate humid conditions (Salgado et al. 2008). Novas et al. (2014, 2015) indicated that "the dinosaur fossils consists of isolated bones of big sauropod dinosaurs, fragmentary remains of a large carnivore and mainly numerous specimens of a new theropod (*C. diegosuarezi*) represented by very complete skeletons, mostly articulated … This new theropod have teeth in the form of leaves, similar to those of the prosauropod dinosaurs and indicative of an herbivore diet. The cervical vertebrae … are similar to those present in basal theropods … The new taxon does not correspond to any previously documented taxon from the Mesozoic units of Patagonia or from the rest of the world, which favours the idea that it represents a new lineage of theropod dinosaurs." The "combination of features of *Chilesaurus* departs from those recognized in any major dinosaur clade, and represents an extreme example of mosaic convergent evolution" (Novas et al. 2015). The presence of different dinosaur fossils, and the discovery of a bizarre new species among them (*C. diegosuarezi*; Novas et al. 2015), and of crocodiles (Lio et al. 2011), make this a unique site for studying Late Jurassic dinosaurs and crocodiles.

Geochronology

Sample location and analytical techniques

Three samples from the dinosaur-bearing succession assigned to the Toqui Formation exposed south of Lago General Carrera were collected for SHRIMP ion microprobe U–Th–Pb zircon dating at the Australian National University. Mineral separation was carried out at the Geochronology Laboratory of the Servicio Nacional de Geología y Minería, Chile (SERNAGEOMIN) using standard crushing, heavy liquid and paramagnetic procedures. Zircon grains were hand picked from the heavy mineral concentrates, mounted in epoxy together with chips of the Temora reference zircon, sectioned approximately in half and polished. Reflected and transmitted light photomicrographs were prepared for all zircons, as were cathodoluminescence (CL) and scanning electron microscope (SEM) images. The CL images were used to decipher the internal structures of the sectioned grains and to ensure that the ~20 μm SHRIMP spot was wholly within a single age component. The U–Th–Pb analyses were made using SHRIMP II following procedures given in Williams (1998, and references therein). Each analysis consisted of six scans through the mass range, with the Duluth Garbo (FC1) or Temora reference grains analyzed for every three unknown analyses. The data have been reduced using the SQUID Excel Macro of Ludwig (2001). The $^{206}Pb/^{238}U$ ratios were normalized relative to a value of 0.0668 for the Temora reference zircon, equivalent to an age of 417 Ma (see Black et al. 2003) and 0.1859 for the FC1 reference zircons, equivalent to an age of 1099 Ma (see Paces and Miller 1993). Uncertainties in the U–Pb calibrations are given in the data tabulations. Uncertainties given for individual analyses (ratios and ages) are at the one sigma level. Tera and Wasserburg (1972) concordia plots, probability density plots with stacked histograms and weighted mean $^{206}Pb/^{238}U$ age calculations were carried out using ISOPLOT/EX (Ludwig 2003). Weighted mean $^{206}Pb/^{238}U$ age uncertainties are reported at the 95 % confidence limits.

Results

Three new SHRIMP U–Pb zircon dates are presented below in Tables 1, 2, 3 and Fig. 6. In this study we will use the ICS International Chronostratigraphic Chart (Cohen et al. 2013; updated). The samples are discussed below from oldest to youngest:

1. Sample CH-6281 (GPS location 698021/4805763) is of an ignimbrite 15 m thick underlying dinosaur-bearing green conglomerates and sandstones. Nineteen zircon grains were analyzed (Fig. 6a; Table 1). A range of $^{206}Pb/^{238}U$ ages is recorded with a dominant grouping at about 147 Ma. The analysis of grain 16, with a result of 764 Ma, is much older and may represent an inherited zircon probably from a Neoproterozoic basement. A weighted mean for the remaining 18 analyses has no excess scatter giving 147 ± 1.0 Ma. This is interpreted to date igneous zircon crystallization in this felsic volcanic rock.
2. Sample CH-8177 is from an acid tuff, 2 m thick, intercalated in green sandstones with dinosaur fossils (GPS location ca. 698102/4805743). The tuff has been partially eroded and its upper contact is an erosional surface with a conglomeratic sandstone that represents a debris flow deposit. Eighteen zircon grains were analyzed (Fig. 6b; Table 2). They plot close to the Tera–Wasserburg concordia curve at about 149 Ma and mostly form a simple bell-shaped age distribution. A weighted mean of the $^{206}Pb/^{238}U$ ages for the 18 analyses has no excess scatter giving 148.7 ± 1.4 Ma.
3. Sample CH-8199 is of a gray ignimbrite from the upper levels of the lower facies association, exposed to the SW of the other two samples (GPS location 698600/4804097). The dated tuff is a 2-m-thick nonwelded gray ignimbrite, with green pumices that includes fossil bones, and underlies, with an erosional contact, a gray colored conglomeratic succession with lenses of pebbly sandstones. A few meters below the dated ignimbrite there is a finely stratified succession, 5 m thick, of tuffs and tuffites which represents subaqueous deposits. Seventeen zircon grains have been analyzed (Fig. 6c; Table 3). They plot close to the Tera–Wasserburg concordia curve at about 148 Ma and mostly form a simple bell-shaped age distribution. A weighted mean of the $^{206}Pb/^{238}U$ ages for the 17 analyses has no excess scatter giving 147.9 ± 1.5 Ma, and without grain 5, gives an age of 147.8 ± 1.3 Ma.

The three SHRIMP dates ranging from 150.1 to 146 Ma indicate zircon crystallization during the Tithonian.

Conclusions

Three U–Pb SHRIMP zircon dates of 148.7 ± 1.4, 147.9 ± 1.5 and 147.0 ± 1.0 Ma from three tuffs intercalated in a sedimentary succession bearing dinosaur and crocodile fossil bones (Salgado et al. 2008, 2015; Novas et al. 2014), including *C. diegosuarezi*, a new dinosaur taxon (Novas et al. 2015) and assigned to the Toqui Formation (De La Cruz and Suárez 2006), set a Tithonian age for them. The strata bearing the vertebrate fossils include stream flow, debris flow, hyperconcentrated flow deposits, ignimbrites, tuffites and water-lain fall tuffs

Table 1 Summary of SHRIMP U–Pb results for zircon from sample CH6281 (coordinates 698021, 4805763)

Grain spot	U (ppm)	Th (ppm)	Th/U	$^{206}Pb^{*}$ (ppm)	$^{204}Pb/^{206}Pb$	f_{206} (%)	Total				Radiogenic		Age (Ma)	
							$^{238}U/^{206}Pb$	±	$^{207}Pb/^{206}Pb$	±	$^{206}Pb/^{238}U$	±	$^{206}Pb/^{238}U$	±
1.1	522	308	0.59	10.7	0.000346	0.45	42.07	0.51	0.0526	0.0008	0.0237	0.0003	150.8	1.8
2.1	257	164	0.64	5.1	0.001111	0.35	43.46	0.52	0.0518	0.0012	0.0229	0.0003	146.1	1.7
3.1	198	115	0.58	4.0	0.000560	0.59	42.92	0.53	0.0537	0.0014	0.0232	0.0003	147.6	1.8
4.1	474	300	0.63	9.4	0.000360	0.27	43.15	0.48	0.0511	0.0009	0.0231	0.0003	147.3	1.6
5.1	980	454	0.46	19.6	0.000075	0.13	42.91	0.45	0.0501	0.0006	0.0233	0.0002	148.3	1.6
6.1	278	241	0.87	5.6	0.000534	0.57	42.57	0.50	0.0536	0.0013	0.0234	0.0003	148.8	1.7
7.1	791	241	0.30	15.5	0.000104	0.28	43.90	0.47	0.0512	0.0007	0.0227	0.0002	144.8	1.5
8.1	491	283	0.58	9.8	0.000168	0.15	43.02	0.48	0.0502	0.0009	0.0232	0.0003	147.9	1.7
9.1	257	126	0.49	5.5	0.002489	6.36	40.00	0.47	0.0997	0.0020	0.0234	0.0003	149.2	1.8
10	177	67	0.38	3.5	0.000461	0.35	43.30	0.54	0.0518	0.0014	0.0230	0.0003	146.7	1.8
11	465	123	0.27	9.2	0.000315	0.59	43.48	0.48	0.0537	0.0009	0.0229	0.0003	145.7	1.6
12	305	150	0.49	5.8	0.000481	0.59	45.45	0.52	0.0535	0.0021	0.0219	0.0003	139.5	1.6
13	345	199	0.58	6.7	0.000309	0.40	44.24	0.50	0.0521	0.0014	0.0225	0.0003	143.5	1.6
14	1146	792	0.69	23.1	0.000101	0.29	42.60	0.44	0.0514	0.0005	0.0234	0.0002	149.1	1.5
15	373	237	0.63	7.4	0.000077	0.19	43.29	0.49	0.0505	0.0010	0.0231	0.0003	147.0	1.7
16	504	227	0.45	54.6	0.000055	0.33	7.92	0.08	0.0674	0.0004	0.1259	0.0014	764.2	7.8
17	347	152	0.44	6.9	0.000877	0.42	43.38	0.50	0.0523	0.0011	0.0230	0.0003	146.3	1.7
18	513	245	0.48	10.1	0.000469	0.97	43.53	0.48	0.0567	0.0009	0.0228	0.0003	145.0	1.6
19	167	62	0.37	3.3	0.000438	1.14	43.09	0.55	0.0580	0.0016	0.0229	0.0003	146.2	1.9

* Radiogenic 206 Pb

1. Uncertainties given at the one σ level

2. Error in Temora reference zircon calibration was 0.25 % for the analytical session (not included in above errors but required when comparing data from different mounts)

3. f_{206} % denotes the percentage of ^{206}Pb that is common Pb

4. Correction for common Pb made using the measured $^{238}U/^{206}Pb$ and $^{207}Pb/^{206}Pb$ ratios following Tera and Wasserburg (1972) as outlined in Williams (1998)

Age	±no std		±include std
147.0	1.0	0.69	1.0

Table 2 Summary of SHRIMP U–Pb results for zircon from sample CH-8177 (coordinates 698102, 4805743)

Grain spot	U (ppm)	Th (ppm)	Th/U	$^{206}Pb^{*}$ (ppm)	$^{204}Pb/^{206}Pb$	f_{206} (%)	Total				Radiogenic		Age (Ma)	
							$^{238}U/^{206}Pb$	±	$^{207}Pb/^{206}Pb$	±	$^{206}Pb/^{238}U$	±	$^{206}Pb/^{238}U$	±
1.1	416	153	0.37	8.4	0.000306	0.23	42.65	0.51	0.0508	0.0010	0.0234	0.0003	149.1	1.8
2.1	320	117	0.37	6.4	–	<0.01	42.69	0.54	0.0488	0.0011	0.0234	0.0003	149.3	1.9
3.1	1529	764	0.50	31.9	0.000058	0.11	41.13	0.44	0.0500	0.0005	0.0243	0.0003	154.7	1.6
4.1	312	201	0.64	6.3	0.000406	0.34	42.81	0.55	0.0517	0.0012	0.0233	0.0003	148.4	1.9
5.1	353	120	0.34	7.1	0.000130	0.30	42.97	0.54	0.0514	0.0011	0.0232	0.0003	147.9	1.8
6.1	730	294	0.40	14.7	0.000149	0.02	42.75	0.48	0.0492	0.0008	0.0234	0.0003	149.0	1.7
7.1	643	421	0.65	13.2	0.000074	<0.01	42.02	0.49	0.0489	0.0008	0.0238	0.0003	151.7	1.7
8.1	538	475	0.88	10.8	0.000218	0.28	42.60	0.51	0.0512	0.0009	0.0234	0.0003	149.2	1.8
9.1	169	20	0.12	3.3	0.001004	0.33	43.52	0.66	0.0516	0.0017	0.0229	0.0004	146.0	2.2
10	493	202	0.41	10.2	0.000000	0.08	41.50	0.50	0.0497	0.0009	0.0241	0.0003	153.4	1.8
11	168	132	0.79	3.4	–	0.20	42.50	0.65	0.0507	0.0022	0.0235	0.0004	149.6	2.3
12	148	60	0.41	3.0	0.000295	0.18	42.65	0.68	0.0505	0.0018	0.0234	0.0004	149.2	2.4
13	321	93	0.29	6.2	0.000079	0.05	44.82	0.60	0.0493	0.0013	0.0223	0.0003	142.2	1.9
14	274	121	0.44	5.7	0.000029	0.28	41.54	0.57	0.0514	0.0014	0.0240	0.0003	152.9	2.1
15	980	483	0.49	20.7	0.000060	0.09	40.64	0.47	0.0499	0.0007	0.0246	0.0003	156.6	1.8
16	659	266	0.40	13.2	0.000000	<0.01	42.85	0.50	0.0480	0.0009	0.0234	0.0003	148.9	1.7
17	1772	672	0.38	35.1	–	0.12	43.37	0.47	0.0499	0.0005	0.0230	0.0003	146.8	1.6
18	676	433	0.64	13.6	0.000070	0.27	42.84	0.50	0.0512	0.0009	0.0233	0.0003	148.3	1.7

* Radiogenic 206 Pb

1. Uncertainties given at the one σ level

2. Error in Temora reference zircon calibration was 0.66 % for the analytical session (not included in above errors but required when comparing data from different mounts)

3. f_{206} % denotes the percentage of ^{206}Pb that is common Pb

4. Correction for common Pb made using the measured $^{238}U/^{206}Pb$ and $^{207}Pb/^{206}Pb$ ratios following Tera and Wasserburg (1972) as outlined in Williams (1998)

Age	±no std		±include std
148.7	1.0	0.94	1.4

Table 3 Summary of SHRIMP U–Pb results for zircon from sample CH-8199 (coordinates 698600, 4804097)

Grain spot	U (ppm)	Th (ppm)	Th/U	$^{206}Pb^{*}$ (ppm)	$^{204}Pb/^{206}Pb$	f_{206} (%)	Total				Radiogenic		Age (Ma)	
							$^{238}U/^{206}Pb$	±	$^{207}Pb/^{206}Pb$	±	$^{206}Pb/^{238}U$	±	$^{206}Pb/^{238}U$	±
1.1	143	53	0.37	2.8	–	0.28	43.69	0.69	0.0512	0.0018	0.0228	0.0004	145.5	2.3
2.1	317	137	0.43	6.3	0.000240	<0.01	43.02	0.55	0.0481	0.0011	0.0233	0.0003	148.3	1.9
3.1	373	158	0.42	7.4	0.000233	0.10	43.15	0.54	0.0498	0.0011	0.0231	0.0003	147.5	1.8
4.1	229	70	0.30	4.5	–	0.29	43.63	0.61	0.0513	0.0014	0.0229	0.0003	145.7	2.0
5.1	1073	315	0.29	22.6	0.000089	0.10	40.70	0.44	0.0500	0.0008	0.0245	0.0003	156.3	1.7
6.1	116	67	0.58	2.3	0.000806	0.34	43.03	0.72	0.0517	0.0021	0.0232	0.0004	147.6	2.5
7.1	394	222	0.56	8.1	0.000273	0.09	41.95	0.53	0.0498	0.0011	0.0238	0.0003	151.7	1.9
8.1	481	230	0.48	9.8	0.000322	0.04	42.36	0.53	0.0494	0.0010	0.0236	0.0003	150.4	1.9
9.1	603	306	0.51	12.3	0.000141	0.13	42.13	0.49	0.0501	0.0009	0.0237	0.0003	151.0	1.8
10	1563	1255	0.80	31.3	–	0.05	42.95	0.46	0.0494	0.0006	0.0233	0.0003	148.3	1.6
11	754	194	0.26	15.0	0.000143	0.32	43.07	0.61	0.0516	0.0008	0.0231	0.0003	147.5	2.1
12	268	112	0.42	5.2	–	0.38	44.16	0.61	0.0519	0.0014	0.0226	0.0003	143.8	2.0
13	428	157	0.37	8.4	–	0.14	43.96	0.56	0.0500	0.0011	0.0227	0.0003	144.8	1.8
14	197	96	0.49	3.9	0.000052	<0.01	43.22	0.65	0.0477	0.0019	0.0232	0.0004	147.7	2.2
15	208	96	0.46	4.0	0.000950	0.34	44.95	0.98	0.0516	0.0017	0.0222	0.0005	141.4	3.1
16	365	148	0.41	7.3	–	0.17	42.77	0.56	0.0503	0.0012	0.0233	0.0003	148.7	1.9
17	386	199	0.52	7.7	0.000106	0.23	42.80	0.55	0.0508	0.0014	0.0233	0.0003	148.6	1.9

* Radiogenic 206 Pb

1. Uncertainties given at the one σ level

2. Error in Temora reference zircon calibration was 0.66 % for the analytical session (not included in above errors but required when comparing data from different mounts)

3. f_{206} % denotes the percentage of ^{206}Pb that is common Pb

4. Correction for common Pb made using the measured $^{238}U/^{206}Pb$ and $^{207}Pb/^{206}Pb$ ratios following Tera and Wasserburg (1972) as outlined in Williams (1998)

Age	±no std		±include std
147.9	1.2	1.05	1.5

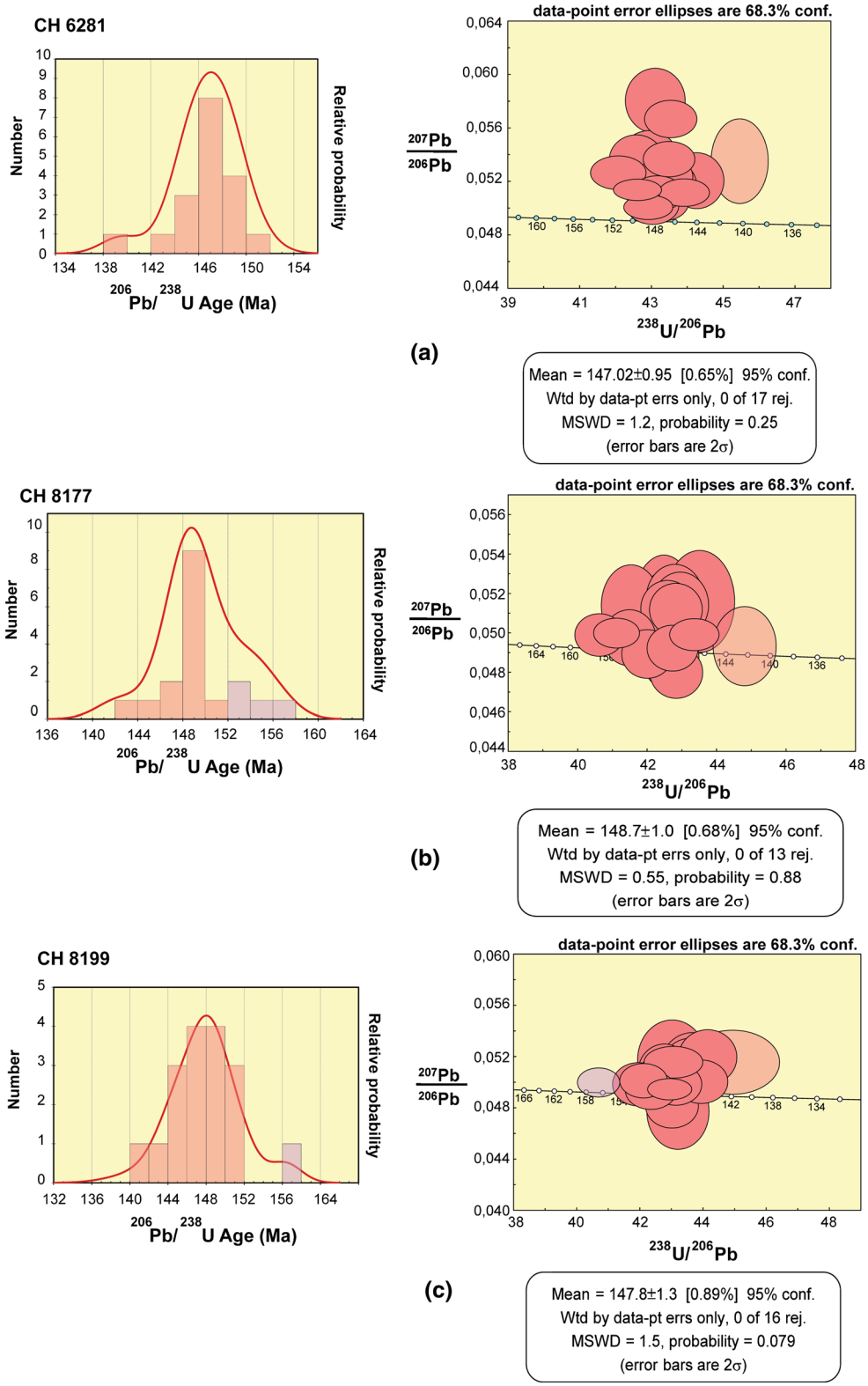

Fig. 6 SHRIMP U–Pb zircon results from samples of the Toqui Formation plotted on Tera and Wasserburg Concordia plots of the total 207Pb/206Pb ratios versus the calibrated 206Pb/238U ratios. *Inset* shows a relative probability plot with stacked histogram for the interpreted magmatic zircon analyses used for the weighted mean age calculation as shown: **a** sample CH-6821; **b** sample CH-8177; **c** sample CH-8199

with interbedded shallow marine glauconite-bearing sandstones. Fossil tree trunks and spores indicate humid condition (Salgado et al. 2008).

The overall depositional setting is that of a fan delta reaching a shallow marine basin, adjacent to active volcanoes rooted on metamorphic rocks. This setting is in

agreement with the synvolcanic Tithonian transgression of the Aysén Basin (De La Cruz et al. 1996; Suárez et al. 2009).

Acknowledgments This work was financed by FONDECYT Projects No. 1121140 (and initiated with FONDECYT projects Nos. 1030162 and 1080516), the Universidad Andres Bello and the Servicio Nacional de Geología y Minería. We acknowledge the curiosity, good sight and capacity of Diego Suárez who at the age of 7 independently discovered the dinosaur fossils, and the assistance of Leonardo Zúñiga, Alvaro Saldivia and Heliberto Leichtle.

References

Aguirre-Urreta MB, Ramos VA (1981) Estratigrafía y paleontología de la Alta Cuenca del Río Roble, provincia de Santa Cruz. 8° *Congreso Geológico Argentino* (San Luis). Actas 3:101–132

Bell CM, Suárez M (1997) The lower cretaceous Apeleg formation of the Aisén basin, southern Chile. Tidal sandbar deposits of an epicontinental sea. Revista Geológica de Chile 24:203–226

Black LP, Kamo SL, Allen ChM, Aleinikoff JN, Davis DW, Kprsch RJ, Foudoulis Ch (2003) Temora 1: a new zircon standard for Phanerozoic U–Pb geochronology. Chem Geol 200(1–2):155–170

Casamiquela R, Corvalán J, Franquesa F (1969) Hallazgo de dinosaurios en el Cretácico Superior de Chile. Su importancia cronológica y estratigráfica. Instituto de Investigaciones Geológicas. Boletín 25:31

Cohen KM, Finney SC, Gibbard PL, Fan J-X (2013) The ICS international chronostratigraphic chart. Episodes 36(3):199–204

De la Cruz R, Suárez M (2006) Geología del área de Puerto Guadal-Puerto Sánchez, Región de Aisén del General Carlos Ibáñez del Campo. Servicio Nacional de Geología y Minería, Carta Geológica de Chile. Serie Geología Básica 95:1–58

De la Cruz R, Suárez M, Belmar M, Quiroz D, Bell M (2003) Geología del área Coihaique-Balmaceda, Región de Aisén del General Carlos Ibáñez del Campo. Servicio Nacional de Geología y Minería, Carta Geológica de Chile, Serie Geología Básica, No. 80, 40 p., 1 mapa escala 1:100.000

De La Cruz R, Suárez M, Covacevich V, Quiroz D (1996) Estratigrafía de la zona de Palena y Futaleufú (43°15'-43°45' Latitud S), X Región, Chile. Congreso Geológico Argentino, No. 13 y Congreso de Exploración de Hidrocarburos, No. 3, Actas 1:417–424

Demant A, Suárez M, De la Cruz R (2007) Geochronology and petrochemistry of Late Cretaceous—(?) Paleogene volcanic sequences from the eastern central Patagonian Cordillera (45o–45o40'S). Revista Geológica de Chile 34:3–21

Demant A, Suárez M, De la Cruz R, Bruguier O (2010) Lower Cretaceous surtseyan volcanoes in the Eastern central Patagonian Cordillera (45°15′–45°40′S): the Baño Nuevo volcanic complex. Geologic Act 8(2):207–219. International Commission on Stratigraphy, 2008. International Stratigraphic Chart, International Commission on Stratigraphy

Iriarte J, Moreno K, Rubilar D, Vargas A (1999) A titanosaurid from the Quebrada La Higuera Formation (Upper Cretaceous), III Región, Chile. Ameghiniana 36:102

Lio G, Novas F, Salgado L, Suárez M, De La Cruz R (2011) First record of a non-marine Crocodylomorph (Archosauria) from the Upper Jurassic of Chile. IV Congreso Latinoamericano de Paleontología de Vertebrados, San Juan, Argentina. Ludwig, K.R. 2001. SQUID 1.02. A User's Manual. Berkeley Geochronology Center Special Publication. No. 2, 19 p

Ludwig KR (2001) SQUID 1.02. A User's Manual: Berkeley Geochronology Center Special Publication No. 2, 2455 Ridge Road, Berkeley, CA 94709, USA

Ludwig KR (2003) User's manual for Isoplot/Ex. Version 3.0. A geochronological toolkit for Microsoft Excel. Berkeley Geochronology Center, Special Publication No. 4, 71 p

Novas FE, Salgado L, Suárez M, De La Cruz R, Isasi M (2014) La Formación Toqui (Jurásico Superior, sur de Chile) y su fauna de dinosaurios. XIX Congreso Geológico Argentino, S7–8, Junio 2014, Córdoba

Novas FE, Salgado L, Suárez M, Agnolin F, Ezcurra M, Chimento N, De La Cruz R, Issi M, Vargas A, Rubilar-Rogers D (2015) An enigmatic plant-eating theropod from the late jurassic of Chile. Nature. doi:10.1038/nature14307

Paces JB, Miller JD (1993) Precise U–Pb ages of Duluth Complex and related mafic intrusions, northeastern Minnesota: geochronological insights to physical, petrogenetic, paleomagnetic, and tectonomagmatic process associated with the 1.1 Ga midcontinent rift system. J Geophys Res 98:13.997–14.013

Rubilar D (2003) Registro de dinosaurios en Chile. Boletín del Museo de Historia Natural 52:137–150

Salgado L, De la Cruz R, Suárez M, Gasparini Z, Fernández M (2008) First late jurassic dinosaurs bones from Chile. J Vertebr Paleontol 28(2):529–534

Salgado L, Novas FE, Suárez M, De La Cruz R, Isasi M, Rubilar-Rogers D, Vaegas A (2015) Upper jurassic sauropods in the Chilean Patagonia. Ameghiniana 52:418–429. doi:10.5710/AMGH.07.05.2015.2883

Salinas P, Sepúlveda P, Marshall L (1991). Hallazgo de dinosaurios (saurópodos) en la Formación Pajonales (Cretácico Superior), Sierra de Almeida, región de Antofagasta, Chile: implicancia cronológica. Resúmenes expandidos del 6° Congreso Geológico Chileno 534–537

Suárez M, De la Cruz R, Bell CM (2007) Geología del Área Ñireguao-Baño Nuevo, Región Aisén del General Carlos Ibáñez del Campo. Servicio Nacional de Geología y Minería, Carta Geológica de Chile, Serie Geología Básica, vol 108, Santiago, pp 1–56

Suárez M, De la Cruz R, Aguirre-Urreta MB, Fanning M (2009) Relationship between volcanism and marine sedimentation in northern Austral (Aisén) Basin, central Patagonia: stratigraphic, U–Pb SHRIMP and paleontologic evidence. J South Am Earth Sci. doi:10.1016/j.jsames.2008.11.009

Suárez M, Demant A, De La Cruz R, Fanning M (2010) Aptian tuff cones during the waning stage of the Aisén Basin, Central Patagonian Cordillera: U–Pb and Ar/Ar dating. J South Am Earth Sci 29:731–737

Suárez M, Márquez M, De La Cruz R, Navarrete C, Fanning M (2014) Cenomanian-?erly Turonian minimum age for the Chubut Group, Argentina: SHRIMP U–Pb geochronology. J South Am Earth Sci 50:67–74

Tera F, Wasserburg G (1972) U–Th–Pb systematics in three Apollo 14 basalts and the problem of initial Pb in lunar rocks. Earth Planet Sci Lett 14:281–304

Williams IS (1998) U-Th–Pb geochronology by ion microprobe. Rev Econ Geol 7:1–35